RECOMMENDATION ITU-R P.1621

Propagation data required for the design of Earth-space systems operating between 20 THz and 375 THz

(Question ITU-R 228/3)

(2003)

The ITU Radiocommunication Assembly,

considering

a)   that the spectrum between 20 THz and 375 THz is available for communications in near-Earth and deep space environments;

b)   that for the proper planning of Earth-space systems operating between 20 THz and 375 THz, it is necessary to have appropriate propagation data;

c)   that methods have been developed that allow the calculation of the most important propagation parameters needed in planning Earth-space systems operating between 20 THz and 375 THz;

d)   that, as far as possible, these methods have been tested against available data and have been shown to yield an accuracy that is both compatible with the natural variability of propagation phenomena and adequate for most present applications in the planning of systems operating between 20 THz and 375 THz,

recognizing

a)   that No. 78 of Article 12 of the ITU Constitution states that a function of the Radiocommunication Sector includes, "… carrying out studies without limit of frequency range and adopting recommendations …",

recommends

1   that the methods for predicting the propagation parameters given in Annex 1 be adopted for planning Earth-space systems, in the respective ranges of validity indicated in the Annex.

NOTE 1 – Supplementary information related to propagation prediction methods for frequencies between 20 THz and 375 THz may be found in Recommendation ITU-R P.1622.

Annex 1

1   Atmospheric considerations

The performance of a system operating in the 20-375 THz frequency range between the Earth and an orbiting spacecraft is affected by the atmosphere of the Earth. These atmospheric effects include:

–   absorption by molecules of atmospheric gasses present along the propagation path resulting in an overall loss in signal amplitude;

–   scattering by particles ranging in size from fractions of a wavelength to many wavelengths present along the propagation path resulting in an apparent loss in signal amplitude;

–   refraction of the beam due to changes in atmospheric density along the propagation path resulting in an apparent movement in the position of the transmitting source;

–   turbulence due to thermal variations in the atmosphere resulting in fluctuations in the received amplitude and phase of the signal.

This Annex deals only with the effects of the troposphere on the wanted signal. As far as possible, the prediction methods in this Annex have been tested against measurements on terrestrial-free space links and astronomical systems. These methods yield results suitable for basic system planning. However, due to the spatial and temporal variability of the atmosphere, local site surveys of propagation characteristics are essential prior to the deployment of any ground-based system operating between 20 THz and 375 THz.
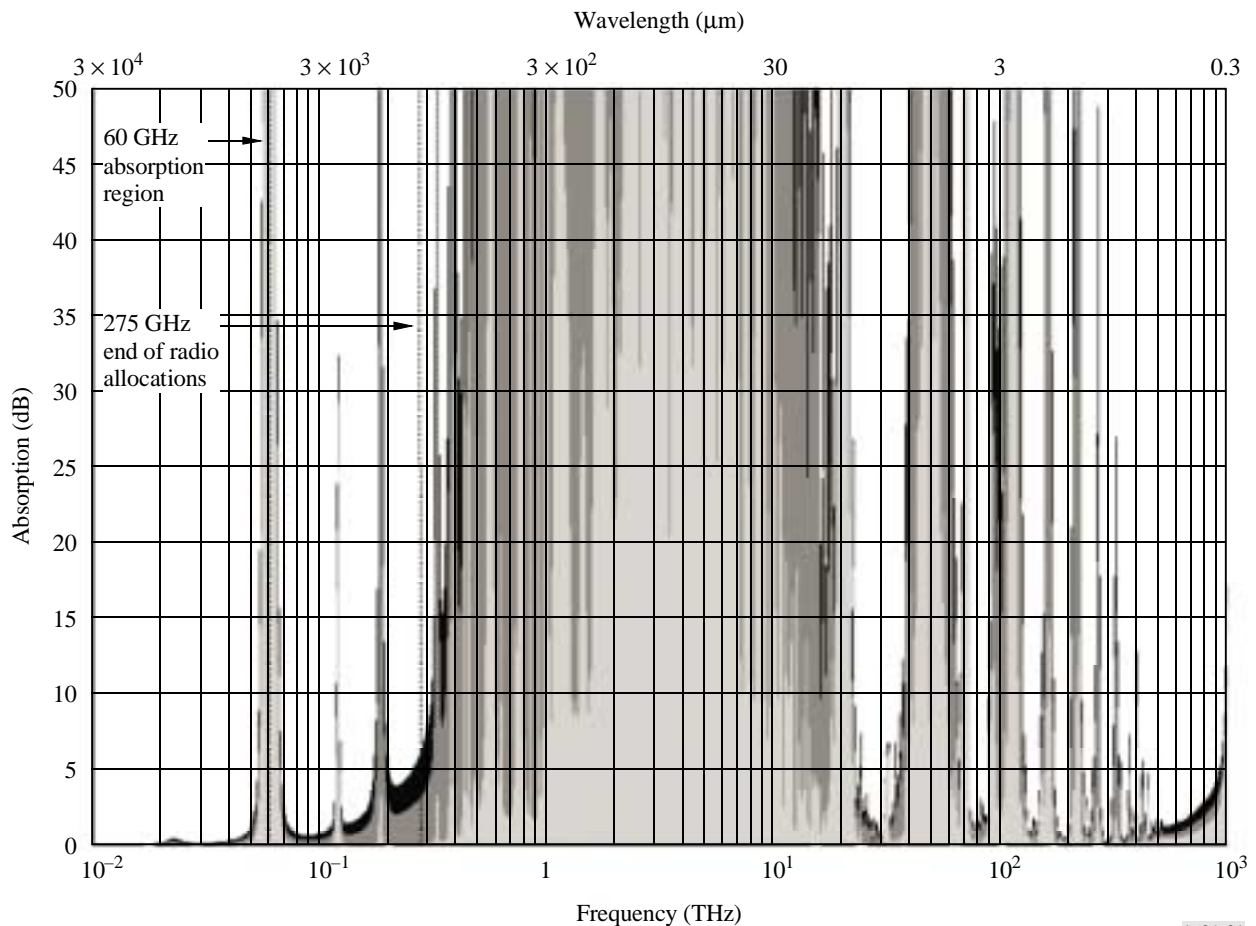
2   Absorption

Figure 1 illustrates the frequency dependence of atmospheric absorption along three zenith paths. The area shaded in light grey illustrates the relatively low absorption associated with a site located 5 km above sea level in an area of low humidity. The darker grey area shows the additional atmospheric absorption that would occur for a site located 2 km above sea level. The black regions show the further impact of atmospheric absorption for a site located at sea level and transmitting through a standard atmosphere as provided in Recommendation ITU-R P.835. The Figure clearly shows that the atmosphere, except at some dry, high altitude locations, is opaque to electromagnetic energy at almost all frequencies between about 1 THz and 10 THz (300 μm and 30 μm). Above 10 THz, the absorptive characteristics of the atmosphere again become favourable to propagating electromagnetic energy between the surface of the Earth and space.

The absorptive characteristics of the spectral region above 10 THz (below 30 μm), shown in detail in Fig. 2 for the same three zenith paths, are characterized by a series of regions of low absorption separated by strong but narrow regions of high absorption. The individual regions of low absorption are limited by a fine structure of many weak absorption lines. Individual absorption lines occur due to the presence of gaseous components in the atmosphere including, but not limited to: NH_3, CO_2, CO, CH_4, NO_2, NO, O_2, O_3, SO_2, H_2O, and various CFCs. The strength of the absorption lines is dependent on temperature and pressure.

Calculations of atmospheric absorption are possible using a line-by-line method similar to Annex 1 of Recommendation ITU-R P.676. However, as thousands of individual lines are present across the spectral range from 10 THz to 1 000 THz (30 μm to 0.3 μm), such a method is computationally intensive.

FIGURE 1

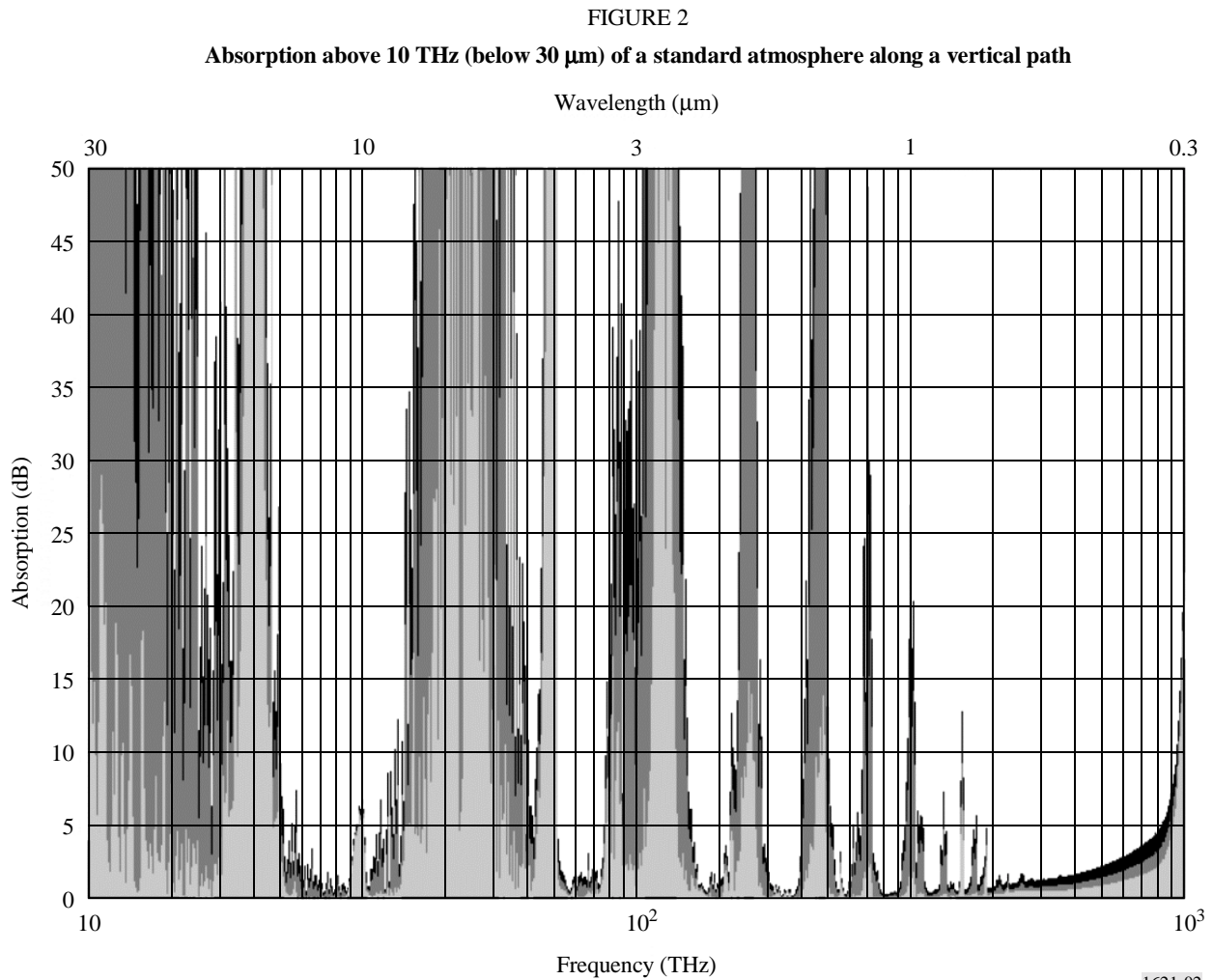**Atmospheric absorption along a vertical path**

3 Scattering

Atmospheric scatter results in an apparent reduction in signal strength at the receiver due to a redirection of the transmitted energy away from the intended propagation path. The scattering characteristics of the atmosphere are dependent on the diameter of the scattering particles present along the propagation path. Scattering characteristics take three forms:

– Rayleigh

– Mie

– Wavelength independent.

3.1 Rayleigh scattering

The atmosphere exhibits Rayleigh scattering characteristics when the scattering particles along the propagation path have a much shorter physical diameter than the wavelength of the electromagnetic wave. At frequencies above 20 THz (wavelength below 15 μm), Rayleigh scattering occurs due to interactions between the electromagnetic wave and polar molecules of atmospheric gases.

FIGURE 2

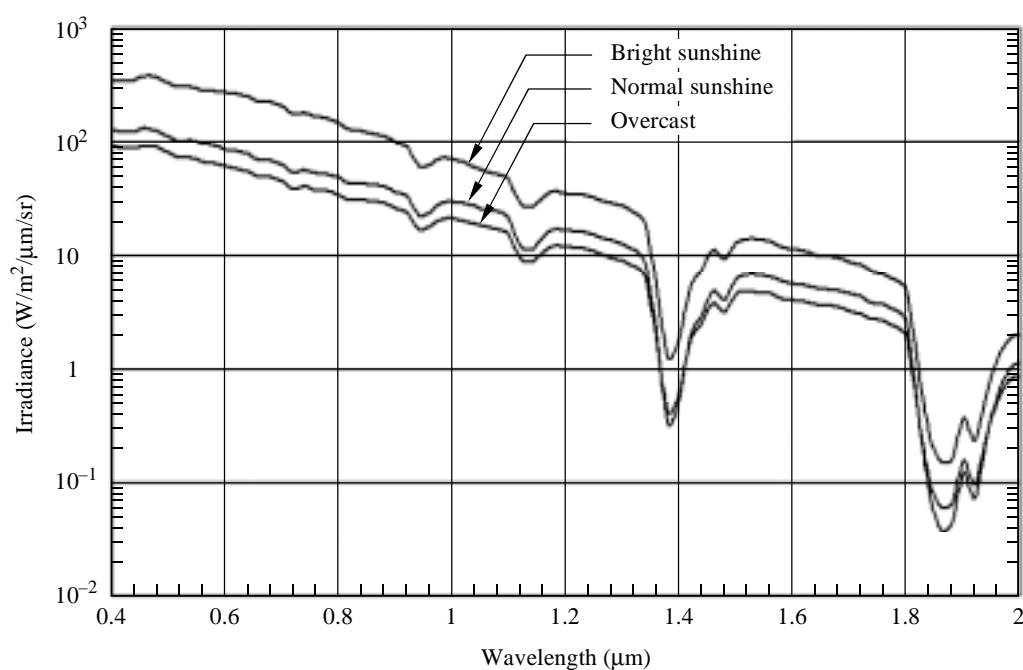**Absorption above 10 THz (below 30 μm) of a standard atmosphere along a vertical path**

The amount of apparent signal loss at the receiver attributable to Rayleigh scattering is negligible for frequencies below 375 THz (wavelength greater than 0.8 μm). However, the magnitude of Rayleigh scattering has a wavelength dependence of λ^{-4}. At about 1 000 THz (0.3 μm) the impact of Rayleigh scattering on a transmitted signal becomes comparable to Mie scattering.

The most significant result of Rayleigh scattering is the introduction of background noise into receivers. Background noise appears along paths in both the Earth-to-space and space-to-Earth directions. The primary noise source for earth stations operating with spacecraft comes from Rayleigh scatter of sunlight during daytime operations. Spacecraft pointed at the Earth will also encounter noise from sunlight reflected from the Earth's surface, although this is not a Rayleigh effect.

Figure 3 provides the radiance, H, of the sky for several conditions each in W/m^2/μm/sr. For simplicity, Table 1 provides specific values of H for the primary frequencies of interest for space-based communication above 20 THz. A reasonable value of H during night-time operations is $\sim 1 \times 10^{-9}$ W/m^2/μm/sr for most frequencies of interest.

FIGURE 3
Radiance of the sky for various sun conditions

1621-03

TABLE 1

Radiance, H (W/m^2/μm/sr), of the sky and Earth for several frequencies

Frequency (THz)	Wavelength (μm)	Sky background		
		Bright sunshine	Normal sunshine	Overcast
566.0	0.530	303.4	101.6	71.75
352.9	0.850	122.3	42.58	30.3
310.9	0.965	64.62	25.12	18.63
283.0	1.06	54.45	25.32	17.99
200.0	1.50	13.01	6.00	4.44

The background noise power, P_{back}, arriving at the receiver is given by:

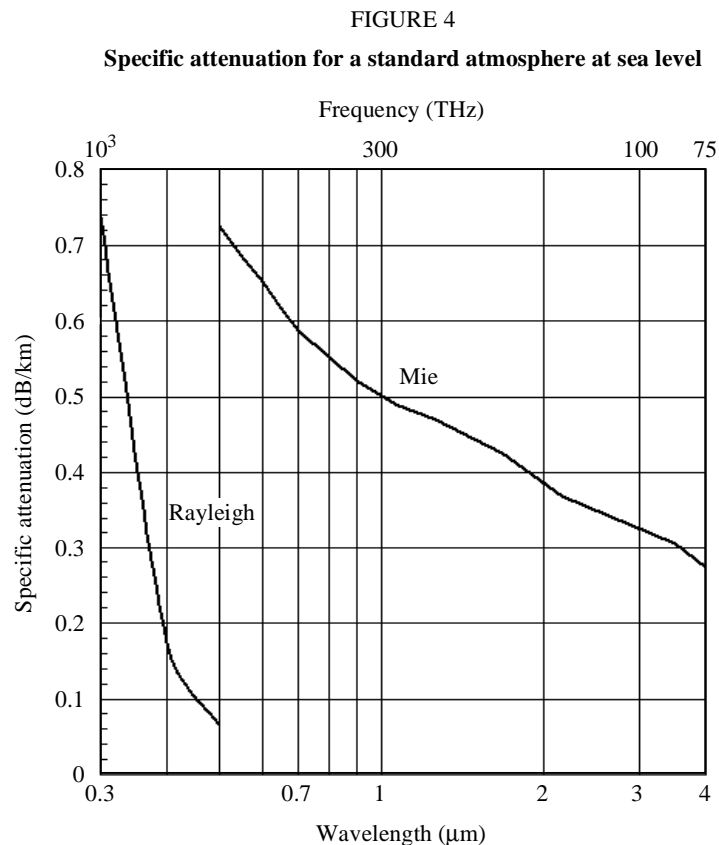$$P_{back} = \frac{\pi \theta_r^2 \, A_r \, \Delta\lambda H}{4} \qquad \text{W} \qquad (1)$$

where:

θ_r: field of view of the receiver (rad)

A_r: area of the receiver (m^2)

$\Delta\lambda$:   bandwidth of the receiver (μm)

H: radiance (W/m^2/μm/sr).

Apart from background noise due to Rayleigh scatter, other sources of background noise may also appear. These sources include but are not limited to planets, bright stars, and reflections from natural or artificial objects. During periods of intense rain, systems operating between 20 THz and 375 THz are not considered operational. Therefore, lightening is not considered a noise source along Earth-space paths. Depending on the orientation and motion of the propagation path as well as that of background noise sources, the magnitude and duration of noise events may vary by many orders of magnitude.

3.2   Mie scattering

The atmosphere exhibits Mie scattering characteristics when the scattering particles along the propagation path have roughly the same physical diameter as the wavelength of the electromagnetic wave. Mie scattering is a complex function of the size, shape and number of particles along the propagation path. The distribution of particle sizes and shapes along the propagation path are a function of the path profiles of both water vapour content and wind speed. Aerosols and microscopic water particles are the predominant components of Mie scattering at frequencies between 20 THz and about 375 THz (15 μm and 0.8 μm). In this frequency range, Mie scattering is a significantly greater effect than Rayleigh scattering. For comparison, Fig. 4 shows the specific attenuation (dB/km) of Rayleigh and Mie scattering for a standard atmosphere at sea level.

FIGURE 4

Specific attenuation for a standard atmosphere at sea level

1621-04

3.3 Wavelength independent scattering

The atmosphere exhibits wavelength independent scattering characteristics when the scattering particles along the propagation path have a much larger physical diameter than the wavelength of the electromagnetic wave. Wavelength independent scattering is most accurately described by diffraction theory.

The particles most frequently occurring on Earth-space paths are hydrosols and hydrometeors. The effects of wavelength independent scattering are significant. Clouds, fog, rain, or snow can effectively prohibit the propagation of electromagnetic radiation above 20 THz (below 15 μm).

4 Refraction

Atmospheric refraction occurs when electromagnetic energy propagates through media with varying densities. The effect on a system operating between 20 THz and 375 THz along an Earth-space path is an angular shift in the direction of the propagation path. Refraction is a function of wavelength and elevation angle as well as the temperature and pressure profile along the propagation path.

4.1 Formula for the effective atmospheric refractive index

The effective atmospheric refractive index, n_{eff}, for frequencies above 150 THz (wavelengths < 2 μm) at temperature $T = 15°$ C and pressure $P = 1\,013.25$ hPa for a vacuum wavelength, λ_{vac}, is approximated by:

$$n_{eff} = 1 + 10^{-8}\left(6\,432.8 + \frac{2\,949\,810}{146 - \lambda_{vac}^{-2}} + \frac{25\,540}{41 - \lambda_{vac}^{-2}}\right)$$

(2)

where:

λ_{vac}: wavelength (μm).

The effective atmospheric refractive index can be adjusted for other temperatures and pressures using the expression:

$$n_{eff}(T,P) = 1 + (n_{eff} - 1)\,\frac{1.162P(1 + P(0.7868 - 0.0113T)10^{-6})}{760.4696(1 + 0.0366T)}$$

(3)

where:

T: temperature (ºC)

P: atmospheric pressure (hPa).

Water vapour has only a very slight influence (less than 1%) on the atmospheric refractive index in the frequency range mentioned above.

The effective atmospheric refractive index, n_{eff}, differs from the actual atmospheric refractive index, n, by taking into account the vertical path profile. The value of n_{eff} allows calculations of the apparent change in elevation angle to be conducted using Snell's law as given in (4). The use of n_{eff} is satisfactory because, in practice, values of n present along the propagation path will fluctuate rapidly. The acquisition and tracking systems must automatically adjust in real-time to account for these fluctuations. Therefore, systems operating between 150 THz and 375 THz only require an approximation for the initial acquisition.

4.2   Apparent change in elevation angle

Refraction will cause the apparent elevation angle to a spacecraft to differ from its true elevation angle. The amount of refraction occurring in the atmosphere is calculated using Snell's law and the value of n_{eff} calculated in (2) and (3). The observed elevation angle is calculated by:

$$\theta_{obs} = \cos^{-1}\left(\frac{\cos(\theta_t)}{n_{eff}(T,P)}\right) \tag{4}$$

where:

θ_{obs} :   observed elevation angle

θ_t :   true elevation angle

$n_{eff}(T,P)$:   effective atmospheric index of refraction.

Equation (4) is based on the assumption that the Earth's atmosphere has uniform thickness and a constant temperature and pressure with a refractive index $n_{eff}(T,P)$.

5   Turbulence

Turbulence arises due to parcels of air with varying refractive indices present along the propagation path. The parcels (i.e. turbulent cells) may vary in size from a few millimetres to tens of metres with many different sizes simultaneously present along the path. At frequencies between 20 THz and 375 THz, the refractive index of a cell is driven by temperature rather than humidity as is the case for traditional radio frequencies (i.e. frequencies arbitrarily less than 3 000 GHz). The effects of thermally induced turbulence are different in the Earth-to-space and space-to-Earth directions.

5.1   Measures of turbulence

There are four measures of atmospheric turbulence that collectively describe the propagation characteristics present along a slant path. These parameters are:

C_n^2 :   a height dependent measure of the strength of atmospherically induced turbulence ($m^{-2/3}$);

r_0 :   the coherence length of the atmosphere describes the effective diameter of a single aperture receiving energy that has propagated through atmospheric turbulence (m);

θ_0 :   the isoplanatic angle of the atmosphere is the angular range over which a portion of the wavefront, having passed through atmospheric turbulence is correlated to a specified degree – typically 1 (rad);

τ_0 :   the critical time constant of the atmosphere describes the temporal rate of variations in the turbulence along the propagation path (s).

5.1.1 Turbulence structure parameter, C_n^2

The method described below is based on the Huffnagel-Valley 5/7 model. The model was developed for night-time applicability and can be used to calculate the turbulence structure parameter, C_n^2, along a slant path. The following parameters are required:

v_g: ground wind speed (m/s);

C_0:   nominal value of C_n^2 at ground level (typically $\sim 1.7 \times 10^{-14}$ m$^{-2/3}$).

Step 1: Calculate the r.m.s. wind speed along the vertical path, v_{rms}, using a form of the Bufton wind model simplified for the GSO case, from:

$$v_{rms} = \sqrt{v_g^2 + 30.69 v_g + 348.91} \qquad \text{m/s} \tag{5}$$

When the ground wind speed is unknown, a value of $v_g = 2.8$ m/s may be used as an approximation resulting in $v_{rms} = 21$ m/s.

Step 2: Calculate the turbulence structure parameter, C_n^2, at height, h, from:

$$C_n^2(h) = 8.148 \times 10^{-56} v_{rms}^2 h^{10} \exp^{-h/1000} + 2.7 \times 10^{-16} \exp^{-h/1500} + C_0 \exp^{-h/100} \qquad \text{m}^{-2/3} \tag{6}$$

where:

         h: height above ground level (m).

This model for C_n^2 can be applied for general system planning for any point on Earth. However, C_n^2 will vary significantly from location to location. A knowledge of local C_n^2 characteristics is essential prior to system development. C_n^2 also varies considerably with height at the lowest heights above ground. Therefore, to ensure an accurate estimate of the atmospheric turbulence profile, h should increase exponentially, from 0.001 km at the lowest layer (ground level) to 1 km at an altitude of 20 km, according to the following equation:

$$h_i = \exp\left\{\frac{i-1}{20}\right\} \qquad \text{m} \tag{7}$$

from $i = 1$ to 139, noting that $h_{139} \cong 1\,000$ m and $\sum_{i=1}^{139} h_i \cong 20$ km.

Figure 5 shows C_n^2 is greatest at the surface and decreases rapidly with increasing height. At around 10 km above the ground, C_n^2 increases slightly but falls off steeply. The value of C_n^2 is most dependent on C_0 at low heights. The effects of wind have the greatest impact on C_n^2 at heights above about 1 km. C_n^2 becomes negligible at heights greater 20 km above the Earth's surface.

5.1.2 Atmospheric coherence length

The coherence length of the atmosphere, r_0, describes the effective diameter, due to turbulence, of a single, diffraction limited, fixed aperture, and is illustrated in Fig. 6. A fixed aperture with a diameter less than or equal to r_0 will collect energy from a coherent portion of the wavefront. A fixed aperture larger than r_0 will receive a degraded wavefront across its surface.
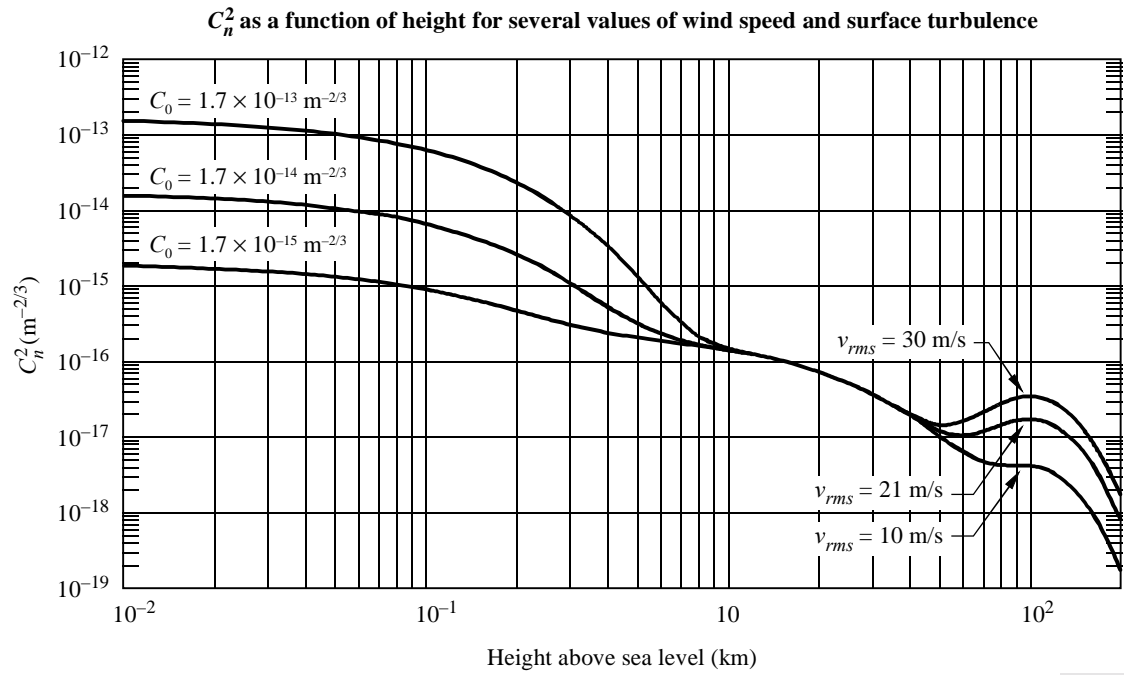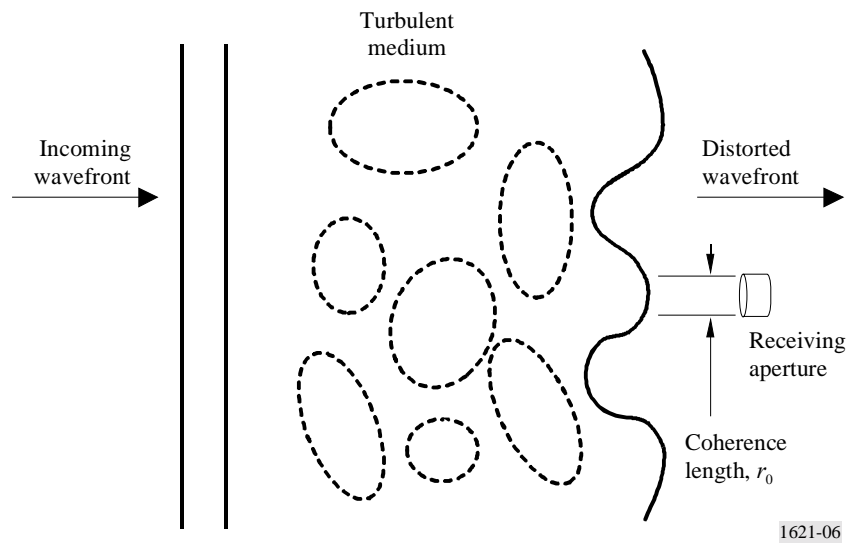
FIGURE 5

C_n^2 as a function of height for several values of wind speed and surface turbulence

1621-05

FIGURE 6

Coherence length

1621-06

Coherence length is traditionally calculated by:

$$r_0 = \left(0.423 k^2 \sec \zeta \int_{h_0}^{Z} C_n^2(h)\, \mathrm{d}h \right)^{-3/5} \qquad \text{m} \qquad (8a)$$

where:

k: wavenumber (= $2\pi/\lambda$)

ζ: zenith angle

λ: wavelength (m)

h_0: height above ground-level (m).

This is equivalent to:

$$r_0 = \frac{1.1654 \times 10^{-8} \lambda^{1.2} \sin^{0.6}\theta}{\left(\int\limits_{h_0}^{Z} C_n^2(h)\,\mathrm{d}h\right)^{0.6}} \qquad \text{m} \qquad (8b)$$

where:

λ: wavelength (µm)

θ: elevation angle

h_0: height of earth station above ground-level (m)

h: height above ground-level (m)

Z: effective height of the turbulence (typically 20 km).

If local measurements of C_n^2 along the propagation path are unavailable, the general approximation provided in § 5.1.1 may be used. However, the calculation of $\int C_n^2(h)\,\mathrm{d}h$ in the denominator will not have a closed-form solution. In this case, the following numerical formula for r_0 provides a good approximation.

Step 1: Determine the integral of the wind dependent term, C_{wind}, by:

$$C_{wind} = (8.148 \times 10^{-17} v_{rms}^2) \left(0.0026 \left(1 - \exp^{(0.001 h_0^{1.055} - 5)} \right) + 3.587369 \right) \qquad \text{m}^{1/3} \qquad (9)$$

where:

v_{rms}: r.m.s. wind speed (m/s) as given in equation (5)

h_0: height of the earth station above ground-level (m).

Step 2: Determine the integrated height dependent term, C_{height}, by:

$$C_{height} = -6.5594 \times 10^{-19} + 4.05 \times 10^{-13} \exp^{-h_0/1500} \qquad \text{m}^{1/3} \qquad (10)$$

Step 3: Determine the surface turbulence dependent term of the integral, C_{turb}, by:

$$C_{turb} = -C_0(1.383899 \times 10^{-85} - 100 \exp^{-h_0/100}) \qquad \text{m}^{1/3} \qquad (11)$$

where:

C_0: nominal value of C_n^2 at ground level (typically ~ 1.7×10^{-14} m$^{-2/3}$).

Step 4: The integral of the turbulence profile, $\int_{h_0}^{Z} C_n^2(h)\,\mathrm{d}h$, is approximated by:

$$\int_{h_0}^{Z} C_n^2(h)\,\mathrm{d}h \approx C_{wind} + C_{height} + C_{turb} \qquad \mathrm{m}^{1/3} \qquad (12)$$

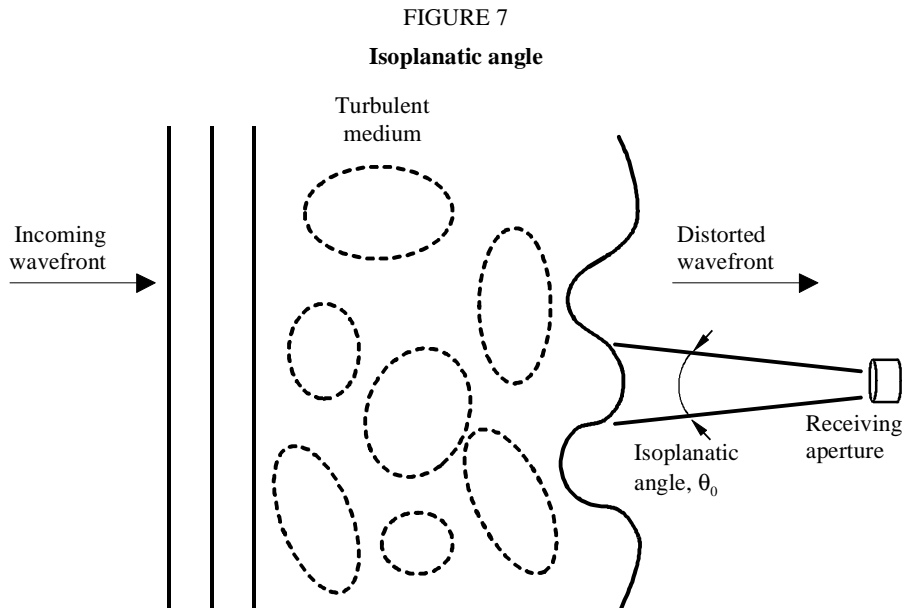*Step 5:* Determine the coherence length, r_0, by:

$$r_0 = \frac{1.1654 \times 10^{-8} \lambda^{1.2} \sin^{0.6}\theta}{(C_{wind} + C_{height} + C_{turb})^{0.6}} \qquad \mathrm{m} \qquad (13)$$

The above formula has been derived as an approximation for an earth station altitude between 0 km and 5 km above sea level and an elevation angle above 45°. The formula assumes that $C_n^2(h)$ becomes negligible at heights greater than 20 km above the Earth's surface.

At frequencies below 30 THz (wavelengths greater than 10 μm), near diffraction limited performance is possible for single aperture systems with a diameter of less than 1 m. The atmospheric coherence length decreases with increasing frequency. For most locations on Earth, r_0 at frequencies above 300 THz (wavelengths less than 1 μm) is on the order of 5 cm however, under excellent conditions, r_0 may be as high as 30 cm.

5.1.3   Isoplanatic angle

Isoplanatic angle, θ_0, which is illustrated in Fig. 7, is the angular range over which a portion of the wavefront, having passed through atmospheric turbulence, is correlated to a specified degree (typically 1 rad). Isoplanatic angles tend to be on the order of 10^{-6} to 10^{-4} rad. The largest values of θ_0 correlate with high elevation angles, low frequencies (long wavelengths), and low values of C_n^2. θ_0 increases almost linearly with frequency (decreasing wavelength) and decreases rapidly with elevation angles below about 75°.

FIGURE 7

Isoplanatic angle

1621-07

Isoplanatic angle is traditionally calculated by:

$$\theta_0 = \left(2.914k^2 \sec^{8/3} \zeta \int_{h_0}^{Z} C_n^2(h)h^{5/3}\, dh \right)^{-3/5} \qquad \text{rad} \qquad (14a)$$

where:

k: wavenumber ($= 2\pi/\lambda$)

ζ: zenith angle

λ: wavelength (m)

h_0: height above ground-level (m).

This is equivalent to:

$$\theta_0 = \frac{3.663 \times 10^{-9} \lambda^{1.2} \sin^{1.6}\theta}{\left(\int_{h_0}^{Z} C_n^2(h)h^{5/3}\, dh \right)^{0.6}} \qquad \text{rad} \qquad (14b)$$

where:

λ: wavelength (μm)

θ: elevation angle

h_0: height of earth station above ground-level (m)

h: height above ground-level (m)

Z: effective height of the turbulence (typically 20 km).

If local measurements of C_n^2 are unavailable, the general approximation provided in § 5.1.1 may be used. However, the calculation of $\int C_n^2(h)h^{5/3}\, dh$ in the denominator will not have a closed-form solution. In this case, the following numerical formula for θ_0 provides a good approximation.

Step 1: Determine the integral of the wind dependent term, C'_{wind}, by:

$$C'_{wind} = 8.148 \times 10^{-10} v_{rms}^2 \left(\left(0.002 \left(1 - \exp^{(0.0018 h_0^{1.014} - 9)} \right) \right) + 2.0043 \right) \qquad \text{m}^2 \qquad (15)$$

where:

v_{rms}: r.m.s. wind speed (m/s) as given in equation (5)

h_0: height of the earth station above ground-level (m).

Step 2: Determine the integrated height dependent term, C'_{height}, by:

$$C'_{height} = -7.0236 \times 10^{-23} h_0^4 + 1.5015 \times 10^{-18} h_0^3 - 8.9834 \times 10^{-15} h_0^2 + 2.3855 \times 10^{-12} h_0 + 9.6181 \times 10^{-8} \quad \text{m}^2 \quad (16)$$

Step 3: Determine the surface turbulence dependent term of the integral, C'_{turb}, by:

$$C'_{turb} = 3.3 \times 10^5 C_0 \exp^{-0.000222 h_0^{1.45}} \qquad \text{m}^2 \qquad (17)$$

where:

C_0:   nominal value of C_n^2 at ground level (typically ~ 1.7×10^{-14} m$^{-2/3}$).

Step 4: Determine the isoplanatic angle, θ_0, by:

$$\theta_0 = \frac{3.663 \times 10^{-9} \lambda^{1.2} (\sin \theta)^{1.6}}{(C'_{wind} + C'_{height} + C'_{turb})^{0.6}} \qquad \text{rad} \tag{18}$$

The above formula has been derived as an approximation for an earth station located between 0 km and 5 km above sea level and an elevation angle greater than 45°. Note that $C_n^2(h)$ becomes negligible at heights greater than 20 km above the Earth's surface.

5.1.4   Turbulence temporal characteristics

The temporal characteristics of turbulence are defined with a critical time constant, τ_0, which is the response time required to mitigate the effects of turbulence. The value of τ_0 is related to a parameter in common use, f_G. The relationship between the parameters is $\tau_0 = 1/f_G$. The method described below can be used to calculate τ_0 on slant paths with elevation angles greater than 45°. The following parameters are required:

v_g: wind speed at earth station (m/s)

λ: wavelength (μm)

θ: elevation angle.

Step 1: Obtain the vertical wind velocity profile, $v(h)$. If local measurements of $v(h)$ are not available, it may be approximated by:

$$v(h) = v_g + 30 \exp^{-\left(\frac{h - 9\,400}{4\,800}\right)^2} \qquad \text{m/s} \tag{19}$$

where:

h: height above ground (m).

If local measurements of v_g are not available, a typical value of 2.8 m/s may be assumed.

Step 2: Calculate the integrated wind-weighted turbulence by:

$$v_{5/3} = \int_{h_0}^{Z} C_n^2(h)\,(v(h))^{5/3}\,dh \qquad \text{m}^2/\text{s}^{5/3} \tag{20}$$

where:

$C_n^2(h)$:   turbulence profile

h_0:   height of earth station above ground-level (m)

h: height above ground (m)

Z: effective height of the turbulence (typically 20 km).

If local measurements of C_n^2 along the propagation path are unavailable, the general approximation provided in § 5.1.1 may be used.
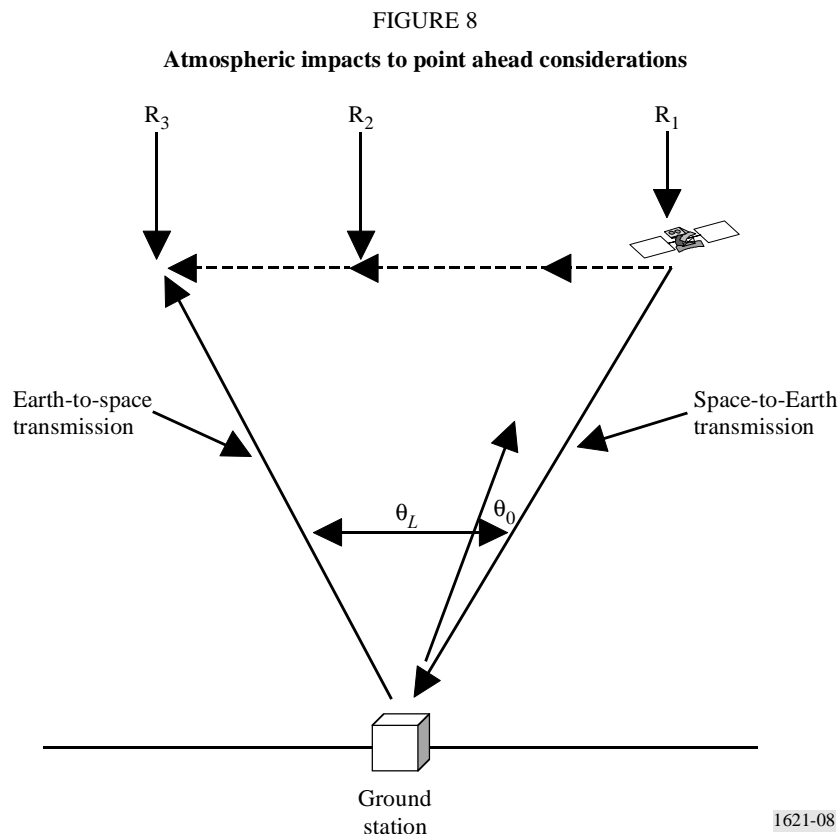
Step 3: Calculate the critical time constant of the atmosphere, τ_0, by:

$$\tau_0 = \frac{2.729 \times 10^{-8} \lambda^{1.2} \sin^{0.6} \theta}{v_{5/3}^{0.6}} \qquad \text{s} \qquad (21)$$

5.1.5   Velocity aberrations

The combination of the propagation delay between a spacecraft and an earth station and the narrow beams possible with systems operating between 20 THz and 375 THz require a transmission in the Earth-to-space direction and a transmission in the space-to-Earth direction between the same two stations to occur along two different propagation paths. Velocity aberrations negate the benefits of some atmospheric compensation techniques when the point-ahead angle, θ_L, is greater than the isoplanatic angle, θ_0.

Figure 8 illustrates the condition under consideration. The spacecraft transmits at point R_1 and, when received on Earth, defines a vector to the satellite position when it was transmitted. However, at the time of reception the satellite has moved to point R_2. When the earth station transmits to the spacecraft, it must compensate for the motion from R_1 to R_2 and for an additional motion-to-point R_3 during the propagation delay.

FIGURE 8

Atmospheric impacts to point ahead considerations

1621-08

A simplified expression for θ_L, when θ_L is assumed to be small, is given by:

$$\theta_L = \frac{2(v_S - v_E)}{c} \qquad \text{rad} \qquad (22)$$

where:

v_S: tangential velocity of the satellite (m/s)

v_E: tangential velocity of the earth station (m/s)

c: speed of light ($\approx 3 \times 10^8$ m/s).

For an earth station on the equator and a GSO satellite at zenith, the point ahead angle is 17.4 μrad. For a non-GSO spacecraft, the point-ahead angle is typically on the order of 50 μrad. This is greater than a typical value of θ_0 within which phase distortions are highly correlated. Thus a correction for the degraded wavefront along the path in the space-to-Earth direction would not be applicable to correcting turbulence along the path in the Earth-to-space direction.